# Evidence for transition of Fermi-surface topology in highly doped $Na_xCoO_2$

T. Arakane,[1] T. Sato,[1] T. Takahashi,[1,2] T. Fujii,[3] and A. Asamitsu[3]
[1]*Department of Physics, Tohoku University, Sendai 980-8578, Japan*
[2]*WPI Research Center, Advanced Institute for Materials Research, Tohoku University, Sendai 980-8577, Japan*
[3]*Cryogenic Center, University of Tokyo, Tokyo 113-0032, Japan*
(Received 11 February 2010; published 22 March 2010)

We have performed angle-resolved photoemission spectroscopy of $Na_xCoO_2$ ($x$=0.65 and 0.77) to clarify the origin of antiferromagnetic (AF) transition. We determined the electronic band structure along the out-of-plane direction by varying photon energy, and revealed that a three-dimensional electron pocket emerges at Γ point in the AF sample ($x$=0.77) while it is absent in the non-AF counterpart ($x$=0.65), showing the transition of Fermi-surface topology with the band filling. The present result suggests that the emergence of the electron pocket is closely related to the various anomalies of the physical properties in Na-rich cobaltates.

DOI: 10.1103/PhysRevB.81.115132 PACS number(s): 71.18.+y, 71.30.+h, 73.20.At, 71.20.Be

## I. INTRODUCTION

After the discovery of superconductivity in hydrated layered cobalt oxides ($Na_xCoO_2 \cdot yH_2O$),[1] intensive theoretical and experimental investigations have been performed to elucidate the physical properties and their relation to the superconductivity. A key to understand the physical properties lies in the two-dimensional (2D) conducting $CoO_2$ layers where the magnetic ground state is expected to be complicated owing to the formation of a geometrically frustrated triangular lattice. The coupling of the magnetic states with the electronic states near the Fermi level ($E_F$) would lead to rich physical properties as a function of band filling. The interplay between the magnetic ordering/fluctuations and the superconductivity is one of the central issues not only in this material but also in various materials such as cuprates, heavy fermions, and iron pnictides.

Nonhydrated $Na_xCoO_2$ exhibits a variety of fascinating physical properties such as the large thermoelectric power,[2,3] the metal-insulator transition accompanied with the charge ordering at $x$=0.5,[4,5] and the antiferromagnetic (AF) transition at $x>0.75$.[6–10] In particular, the AF transition in the highly doped region has attracted a special attention. In the AF phase, Co spins are ferromagnetically aligned in the plane and stacked antiferromagnetically along the $c$ axis.[11–13] The interlayer magnetic correlation is markedly strong as compared to other layered materials,[12,13] suggesting an essentially three-dimensional (3D) nature of the magnetism, whereas the mechanism to trigger such an anomalous AF state as well as its relationship to the charge dynamics has not been well understood. It is thus indispensable to determine band structure and Fermi surface in the highly Na-doped region to obtain an insight into the microscopic origin of the AF transition. By taking into account the noticeably strong out-of-plane magnetic correlations, it is of particular importance to experimentally determine the electronic structure along the $c$ axis.

In this paper, we report results of angle-resolved photoemission spectroscopy (ARPES) of $Na_xCoO_2$ ($x$=0.65 and 0.77) with synchrotron radiation. We determined the 3D Fermi surface (FS) and band dispersions by use of the tunability of photon energy and demonstrate that the FS topology shows a transition upon Na doping. We compare the experimental results with the theoretical predictions and discuss the observed anomalous physical properties.

## II. EXPERIMENTS

High-quality single crystals of $Na_xCoO_2$ ($x$=0.65 and 0.77) were grown by the floating zone method. We have confirmed the AF transition of $Na_{0.77}CoO_2$ at $T_N$=22 K by the magnetic susceptibility and heat-capacity measurements. ARPES measurements were performed with a VG-SCIENTA SES2002 spectrometer at a beamline BL28A at Photon Factory (KEK). We used circularly polarized light of 50–100 eV. The energy and angular resolutions were set at 15–50 meV and 0.2°, respectively. Clean surfaces for ARPES measurements were obtained at *in situ* cleaving of crystal in an ultrahigh vacuum of $1\times10^{-10}$ Torr. The Fermi level ($E_F$) of the sample was referenced to that of a gold film evaporated onto the sample substrate.

## III. RESULTS AND DISCUSSION

Figure 1 shows the plot of ARPES intensity at $E_F$ as a function of in-plane wave vectors $k_x$ and $k_y$ for (a) $Na_{0.77}CoO_2$ (AF sample) and (b) $Na_{0.65}CoO_2$ (non-AF sample) measured with circularly polarized 60 eV photons at $T$=25 K (above $T_N$). In both cases, we immediately notice a large $a_{1g}$ FS centered at $k_x=k_y=0$ as predicted by the local-density approximation band calculation,[14,15] while a theoretically predicted small $e_g'$ hole pocket near K(H) point is absent, consistent with previous ARPES reports.[16–21] As highlighted in Fig. 1(c), the in-plane FS for $x$=0.77 is slightly smaller than that for $x$=0.65 due to the additional electron doping into the $CoO_2$ plane.

To clarify the FS shape along the out-of-plane direction ($k_z$ direction), we measured the photon-energy dependence of ARPES spectrum in the ΓALM plane of the Brillouin zone (BZ). The ARPES intensity plotted as a function of $k_x$ and binding energy is shown in Fig. 2 for several representative photon energies. At $h\nu$=55 and 65 eV for the $x$=0.77 sample, we identify a well-known holelike $a_{1g}$ band which crosses $E_F$ at $k_x\approx-0.6$ Å$^{-1}$. In sharp contrast, the band dis-

 

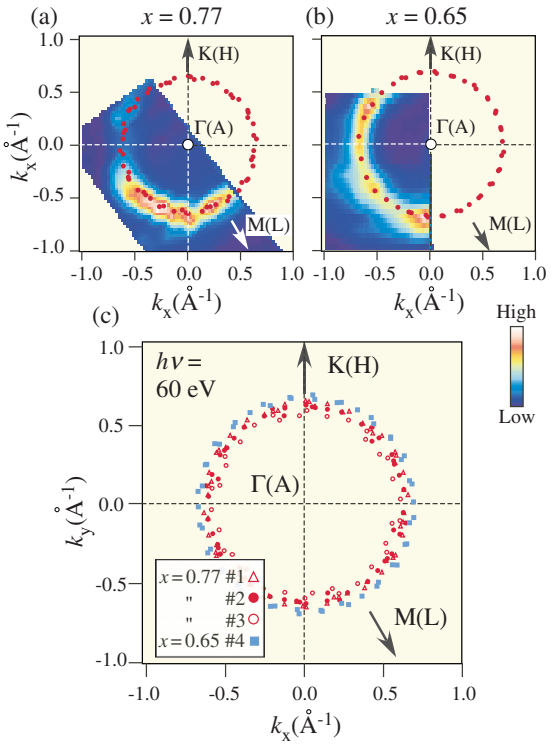


FIG. 1. (Color online) Plots of ARPES intensity at $E_F$ as a function of in-plane wave vectors measured with $h\nu$=60 eV at $T$=25 K for (a) $Na_{0.77}CoO_2$ (AF sample) and (b) $Na_{0.65}CoO_2$ (non-AF sample). ARPES intensity is integrated over the energy range of ±2 meV with respect to $E_F$. Circles represent the position of Fermi vectors ($k_F$) determined by tracing the intensity maxima at $E_F$. The $k_F$ points are symmetrized by assuming a sixfold symmetry with respect to the zone center. (c) Comparison of experimentally determined $k_F$ points between $Na_{0.77}CoO_2$ [red (dark gray) symbols for three samples #1–3] and $Na_{0.65}CoO_2$ [blue (light gray) squares]. Right panel shows the 3D BZ.

persion measured with $h\nu$=70 and 75 eV looks anomalous: besides the $a_{1g}$ band at $k_x \approx -0.45$ Å$^{-1}$, an almost flat band appears in the close vicinity of $E_F$ at $-0.4 < k_x < 0.4$ Å$^{-1}$. Interestingly, this flat band again disappears at $h\nu$=85 eV. These drastic changes upon $h\nu$ variation demonstrate a considerable three dimensionality of the band dispersion. On the other hand, the $h\nu$ dependence of ARPES spectra for $x$=0.65 is substantially different. As shown in Figs. 2(g)–2(k), we observe a single holelike band which crosses $E_F$ but do not find any signatures of a flat band. This indicates that the out-of-plane FS shape is considerably different between the $x$=0.65 and 0.77 samples. To see more clearly the out-of-plane FS shape, we plot in Figs. 2(f) and 2(l) the ARPES intensity at $E_F$ as a function of $k_x$ and $k_z$ for $x$=0.77 and 0.65, respectively. To calculate $k_z$ values, we estimated an inner potential to be 8.0 eV from the periodicity of the band dispersion along the $k_z$ direction. We found that the band dispersions show the periodicity of the single $CoO_2$ layer unit cell rather than that of the double layer, probably because of a weak influence from the periodic potential of O or Na to the near-$E_F$ electronic states. We thus define the notation of high-symmetry points with those of the single-layer unit cell as in the theoretical calculation.[22] As shown in Fig. 2(l), the FS of $x$=0.65 slightly wiggles along the $k_z$ direction, and the $k_F$ position is closest to $k_x$=0 along the ΓM line while it is farthest along the AL line. Such a wiggling is caused by a finite interplane electron hopping. At $x$=0.77, we again find a similar undulating behavior of FS and its amplitude looks much pronounced. Moreover, we identify a sizable ARPES intensity around the Γ point originating in the flat band shown in Figs. 2(c) and 2(d), implying the possible emergence of an additional FS.

To elucidate the FS topology around the Γ point in more detail, we measured ARPES spectra along the near-ΓM cut ($h\nu$=70 eV) with higher resolution. Corresponding energy distribution curves (EDCs) and the intensity at $T$=25 K are

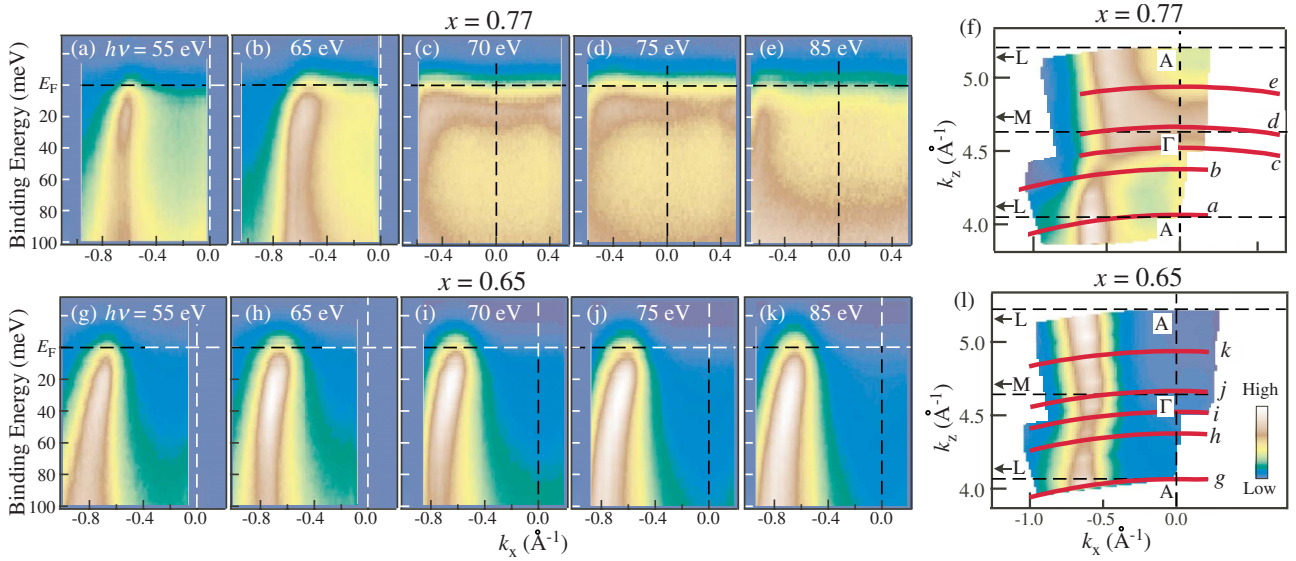


FIG. 2. (Color online) (a)–(e): Photon-energy dependence of the near-$E_F$ ARPES intensity for $Na_{0.77}CoO_2$ plotted as a function of $k_x$ and binding energy measured at $T$=25 K along cuts a–e in the $k_x$-$k_z$ plane as indicated by red lines in (f). (f) ARPES intensity at $E_F$ plotted as a function of $k_x$ and $k_z$. The intensity at $E_F$ is obtained by integrating the spectra within ±2 meV with respect to $E_F$. Red (dark gray) lines show the momentum cuts where the spectra were taken. (g)–(k) and (l): same as (a)–(e) and (f) but for $Na_{0.65}CoO_2$.

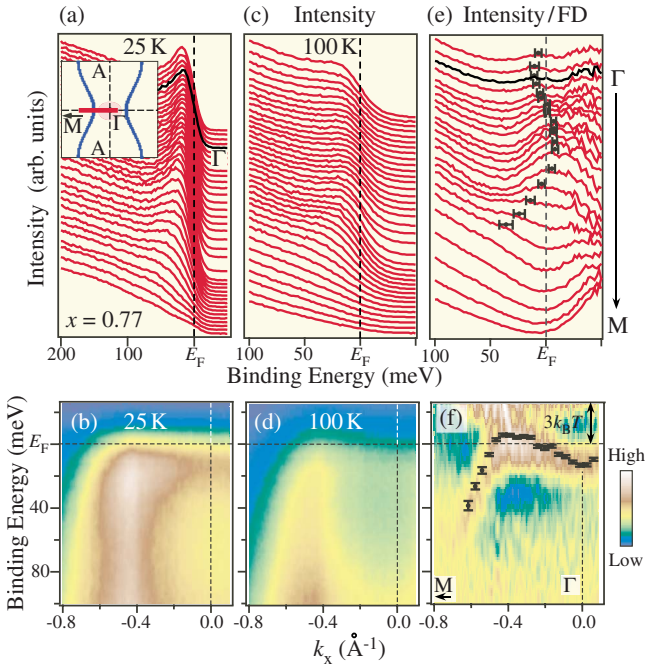


FIG. 3. (Color online) (a) Near-$E_F$ ARPES spectra of $Na_{0.77}CoO_2$ measured at $T=25$ K along the ΓM cut ($h\nu=70$ eV) as shown in the inset. (b) Intensity plot of (a) as a function of $k_x$ and binding energy. (c) and (d): same as (a) and (b) but measured at $T=100$ K. (e) ARPES spectra at $T=100$ K divided by the FD function convoluted with a Gaussian reflecting the instrumental resolution. Black filled circles with error bars correspond to the energy position of the $a_{1g}$ band determined by tracing the peak position of EDCs. (f) Second-derivative intensity plot of (e) as a function of $k_x$ and binding energy. Black filled circles are the same as (e).

plotted in Figs. 3(a) and 3(b), respectively. As seen in Fig. 3(a), a sharp quasiparticle peak is clearly visible at 20 meV below $E_F$ around Γ point. Since this peak may be cutoff by the Fermi-Dirac (FD) distribution function, the actual peak position in the spectral function should be evaluated after removing the effect from the FD function. To do so, we measured ARPES spectra at $T=100$ K along the same cut [Figs. 3(c) and 3(d)]. Although the spectra are thermally broadened, the essential features are still visible [remark the energy scale is different between Figs. 3(a) and 3(c)]. We divided the EDCs by the FD function at $T=100$ K convoluted with a Gaussian reflecting the instrumental resolution as shown in Fig. 3(e) and its second-derivative plot in Fig. 3(f). As visible in Fig. 3(f), the $a_{1g}$ band (black circles) disperses toward $E_F$ on approaching the Γ point from the M point, and crosses $E_F$ at $k_x=-0.45$ Å$^{-1}$. This band has a top of dispersion at 10 meV above $E_F$ at $k_x=-0.4$ Å$^{-1}$ and disperses backward to cross $E_F$ again at $k_x=-0.2$ Å$^{-1}$, giving a characteristic local minimum structure at the Γ point at 15 meV below $E_F$. Concomitantly, an electron pocket appears around the Γ point. In light of the fact that this local minimum structure below $E_F$ is not observed in the $k_z$ region away from the Γ point, it is quite likely that the electron pocket has a closed 3D nature. Apparently, this pocket has an $a_{1g}$ orbital character as in the case of the large hole pocket, since these two FSs originate in the same band.

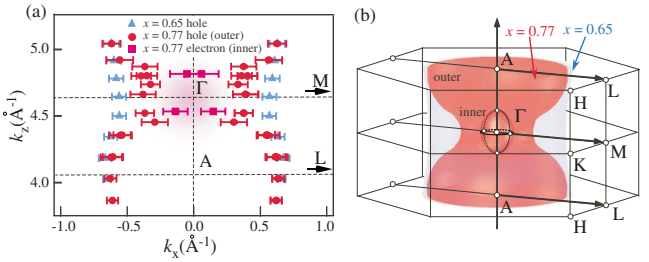


FIG. 4. (Color online) (a) Comparison of experimentally determined $k_F$ points in the $k_x$-$k_z$ plane between $Na_{0.65}CoO_2$ [blue (light gray) triangles] and $Na_{0.77}CoO_2$ [red (dark gray) circles and pink (dark gray) squares]. (b) Schematic view of FS in the 3D BZ for $Na_{0.65}CoO_2$ [blue (light gray)] and $Na_{0.77}CoO_2$ [red (dark gray)].

To evaluate more quantitatively the location and shape of FS, we plot in Fig. 4(a) the experimentally determined $k_F$ points as a function of $k_x$ and $k_z$ for $x=0.65$ and 0.77. Direct comparison of the holelike FS between two compositions reveals that the $k_F$ points nearly coincide with each other around the AL cut ($k_z\approx\pi/2$) while the separation between two $k_F$ points is most significant around the ΓM cut ($k_z\approx0$). This difference is explained as follows. The local maximal point of the $a_{1g}$ band around $k_z=0$ is so close to $E_F$ at $x=0.77$ that even a tiny amount of hole doping dramatically moves the $k_F$ location due to the small Fermi velocity compared to that at $k_z=\pi/2$. Besides such a substantial change in the shape of the cylindrical FS, the doping evolution of the FS around the zone center is dramatic. We do not clearly observe an inner electron pocket at $x=0.65$ unlike $x=0.77$ within the present experimental accuracy. This suggests that the FS topology exhibits an abrupt change upon Na doping at a certain composition of $x\approx0.6$–$0.7$.

Since the out-of-plane FS topology is experimentally established, we roughly estimated the effective doping level $x'$ of the AF sample from the volume of the cylindrical holelike FS and the ellipsoidal electronlike FS ($13.5\pm2.5\%$ and $0.5\pm0.3\%$ of the total volume of the BZ, respectively), by assuming a double degeneracy of the $a_{1g}$ band as well as the circular shape of the in-plane FS at the given $k_z$ value, as illustrated in Fig. 4(b). The estimated value of $x'=0.75\pm0.06$ is in good agreement with the Na content $x=0.77$, suggesting that the Luttinger theorem holds even in the highly doped regime as well as in the lower doping region.[17]

We comment on the differences between the present and previous ARPES works. The observed FS volume consistent with the Luttinger theorem is not in accordance with the previous ARPES results reporting the significant deviation.[19,21] This may be due to the unexpected large $k_z$ band dispersion as revealed in the present work. We also remark that the highly doped bulk samples are unstable and degrade much faster than the lower doping ones. In fact, we recognized that the $a_{1g}$ FS expands and eventually the 3D electron pocket vanishes in aged samples. In the course of ARPES experiments, we thus paid special attention to the sample degradation and measured fresh well-characterized samples soon after the sample growth (within a few weeks). It is also noted that we sometimes observed the doubling of

the holelike $a_{1g}$ band (particularly in the aged samples) which might be regarded as a fingerprint of a "bilayer splitting."[19] However, we observed that only one of two hole pockets disappears after the thermal cycle, suggesting its surface origin.[17] We thus conclude that the bilayer splitting is not clearly visible even in the highly doped region.

Next we discuss the relationship between the 3D electron pocket and various physical properties. The presence of the 3D pocket looks consistent with the fairly large interplane exchange coupling in the AF phase[12,13] and the shrinkage of the *c*-axis length upon Na doping.[23] In the low-doping region, the local minimum of the $a_{1g}$ band is lifted well above $E_F$, leaving a single cylindrical hole pocket at $\Gamma$ point. On the other hand, in the high-doping region around $x \approx 0.77$, the band local minimum is situated below $E_F$ to produce a small electron pocket [see Fig. 3(f)], which contributes to the increase in the density of states at $E_F$. This explains well the enhancement of the electric specific-heat coefficient $\gamma_s$ in Na-rich samples.[24,25] We also think that the enhancement of the thermopower in the high-doping region[3] is the natural consequence of the presence of the electron pocket: the bottom of electronlike band at the $\Gamma$ point is within the energy range of the thermal excitations (10 meV relative to $E_F$ at $x=0.77$, corresponding to $0.4k_BT$ at room temperature), and is expected to give a high thermopower.[26]

Finally we discuss the nature of AF state. It has been intensively argued in the previous literatures whether the spin state in the highly doped region is better characterized by the localized or itinerant picture.[6,8,9,12,13,22,27] A recent 3D Hubbard model calculation within the itinerant spin picture[22] has predicted that the FS becomes more 3D-like in highly doped region since the local minimum structure of the $a_{1g}$ band at the $\Gamma$ point is situated below $E_F$. Noticeably, the ARPES-derived band structure is qualitatively consistent with this prediction, supporting the itinerant nature of the AF state. In this sense, the AF state could be regarded as the spin-density-wave (SDW) state, as also supported by the muon spin rotation and relaxation ($\mu$SR) experiments[7,8] and the metallic conductivity below $T_N$.[4,6,9] Since the SDW generally involves the FS nesting, it is useful to discuss the relationship between the observed FS shape and the nesting vector. According to the neutron-scattering study, the magnetic ordering vector is $Q \approx (0,0,\pi)$.[12,13] There are three possibilities to satisfy the nesting condition via this wave vector, i.e., (i) the intra-FS nesting between the outer quasi-2D pockets, (ii) the same but between the inner 3D pockets, and (iii) the inter-FS nesting between the inner and outer pockets. The possibility (i) would be ruled out since a similar quasi-2D pocket also exists in lower doping non-SDW samples. The scenario (ii) is also unlikely since the 3D pocket is too small to be connected by the nesting vector near $Q=(0,0,\pi)$. In the case of (iii), the nesting which connects the sides of the quasi-2D and the 3D FSs may be possible, while it is necessary to consider the inelastic scattering process incorporating the actual spin-wave dispersion.[12,13]

## IV. SUMMARY

In summary, we have reported high-resolution photon-energy-dependent ARPES results on $Na_xCoO_2$ ($x=0.65$ and 0.77). We have demonstrated that the SDW sample ($x=0.77$) possesses a small 3D electron pocket at the $\Gamma$ point in addition to a quasi-2D hole pocket. The 3D electron pocket is created by the presence of a local minimum structure in the below-$E_F$ band dispersion at the $\Gamma$ point. We have concluded that the various physical anomalies in the highly doped samples are well explained in terms of the transition of the FS topology.

## ACKNOWLEDGMENTS

We thank K. Nakayama, T. Qian, K. Ono, and M. Kubota for their help in the experiment. ARPES measurements were carried out at KEK-PF (Proposal No. 2006S2-001). This work was supported by grants from JSPS, MEXT, and CREST-JST of Japan. T.A. thanks JSPS for a financial support.

[1] K. Takada, H. Sakurai, E. Takayama-Muromachi, F. Izumi, R. A. Dilanian, and T. Sasaki, Nature (London) **422**, 53 (2003).
[2] I. Terasaki, Y. Sasago, and K. Uchinokura, Phys. Rev. B **56**, R12685 (1997).
[3] M. Lee, L. Viciu, L. Li, Y. Wang, M. L. Foo, S. Watauchi, R. A. Pascal, Jr., R. J. Cava, and N. P. Ong, Nature Mater. **5**, 537 (2006).
[4] M. L. Foo, Y. Wang, S. Watauchi, H. W. Zandbergen, T. He, R. J. Cava, and N. P. Ong, Phys. Rev. Lett. **92**, 247001 (2004).
[5] H. W. Zandbergen, M. L. Foo, Q. Xu, V. Kumar, and R. J. Cava, Phys. Rev. B **70**, 024101 (2004).
[6] T. Motohashi, R. Ueda, E. Naujalis, T. Tojo, I. Terasaki, T. Atake, M. Karppinen, and H. Yamauchi, Phys. Rev. B **67**, 064406 (2003).
[7] S. P. Bayrakci, C. Bernhard, D. P. Chen, B. Keimer, R. K. Kremer, P. Lemmens, C. T. Lin, C. Niedermayer, and J. Strempfer, Phys. Rev. B **69**, 100410(R) (2004).
[8] J. Sugiyama, J. H. Brewer, E. J. Ansaldo, H. Itahara, T. Tani, M. Mikami, Y. Mori, T. Sasaki, S. Hébert, and A. Maignan, Phys. Rev. Lett. **92**, 017602 (2004).
[9] B. C. Sales, R. Jin, K. A. Affholter, P. Khalifah, G. M. Veith, and D. Mandrus, Phys. Rev. B **70**, 174419 (2004).
[10] J. L. Luo, N. L. Wang, G. T. Liu, D. Wu, X. N. Jing, F. Hu, and T. Xiang, Phys. Rev. Lett. **93**, 187203 (2004).
[11] A. T. Boothroyd, R. Coldea, D. A. Tennant, D. Prabhakaran, L. M. Helme, and C. D. Frost, Phys. Rev. Lett. **92**, 197201 (2004).
[12] S. P. Bayrakci, I. Mirebeau, P. Bourges, Y. Sidis, M. Enderle, J. Mesot, D. P. Chen, C. T. Lin, and B. Keimer, Phys. Rev. Lett. **94**, 157205 (2005).
[13] L. M. Helme, A. T. Boothroyd, R. Coldea, D. Prabhakaran, A. Stunault, G. J. McIntyre, and N. Kernavanois, Phys. Rev. B **73**, 054405 (2006).
[14] D. J. Singh, Phys. Rev. B **61**, 13397 (2000).
[15] P. Zhang, W. Luo, M. L. Cohen, and S. G. Louie, Phys. Rev.

Lett. **93**, 236402 (2004).
[16] H.-B. Yang, S.-C. Wang, A. K. P. Sekharan, H. Matsui, S. Souma, T. Sato, T. Takahashi, T. Takeuchi, J. C. Campuzano, R. Jin, B. C. Sales, D. Mandrus, Z. Wang, and H. Ding, Phys. Rev. Lett. **92**, 246403 (2004).
[17] H.-B. Yang, Z.-H. Pan, A. K. P. Sekharan, T. Sato, S. Souma, T. Takahashi, R. Jin, B. C. Sales, D. Mandrus, A. V. Fedorov, Z. Wang, and H. Ding, Phys. Rev. Lett. **95**, 146401 (2005).
[18] M. Z. Hasan, Y.-D. Chuang, D. Qian, Y. W. Li, Y. Kong, A. Kuprin, A. V. Fedorov, R. Kimmerling, E. Rotenberg, K. Rossnagel, Z. Hussain, H. Koh, N. S. Rogado, M. L. Foo, and R. J. Cava, Phys. Rev. Lett. **92**, 246402 (2004).
[19] D. Qian, D. Hsieh, L. Wray, Y.-D. Chuang, A. Fedorov, D. Wu, J. L. Luo, N. L. Wang, L. Viciu, R. J. Cava, and M. Z. Hasan, Phys. Rev. Lett. **96**, 216405 (2006).
[20] T. Arakane, T. Sato, T. Takahashi, H. Ding, T. Fujii, and A. Asamitsu, J. Phys. Soc. Jpn. **76**, 054704 (2007).
[21] J. Geck, S. V. Borisenko, H. Berger, H. Eschrig, J. Fink, M. Knupfer, K. Koepernik, A. Koitzsch, A. A. Kordyuk, V. B. Zabolotnyy, and B. Büchner, Phys. Rev. Lett. **99**, 046403 (2007).
[22] K. Kuroki, S. Ohkubo, T. Nojima, R. Arita, S. Onari, and Y. Tanaka, Phys. Rev. Lett. **98**, 136401 (2007).
[23] L. Viciu, J. W. G. Bos, H. W. Zandbergen, Q. Huang, M. L. Foo, S. Ishiwata, A. P. Ramirez, M. Lee, N. P. Ong, and R. J. Cava, Phys. Rev. B **73**, 174104 (2006).
[24] D. Yoshizumi, Y. Muraoka, Y. Okamoto, Y. Kiuchi, J.-I. Yamaura, M. Mochizuki, M. Ogata, and Z. Hiroi, J. Phys. Soc. Jpn. **76**, 063705 (2007).
[25] T. F. Schulze, M. Brühwiler, P. S. Häfliger, S. M. Kazakov, Ch. Niedermayer, K. Mattenberger, J. Karpinski, and B. Batlogg, Phys. Rev. B **78**, 205101 (2008).
[26] K. Kuroki and R. Arita, J. Phys. Soc. Jpn. **76**, 083707 (2007).
[27] M. Gao, S. Zhou, and Z. Wang, Phys. Rev. B **76**, 180402(R) (2007).